Sixth International Symposium on Marine Propulsors
smp'19, Rome, Italy, May 2019

An Experimental Study on Hydrodynamic Performance of Flexible Composite Model Propellers

Chiharu Kawakita

National Maritime Research Institute (NMRI), Tokyo, Japan

ABSTRACT

Marine propellers operating in the wake generate the unsteady propeller fluid forces and cause a hull vibration. The deformations of general metal marine propellers are not considered, because they have enough rigidity. However, marine propeller using the composite material called flexible propeller appeared, by controlling the actively blade deformation in response to load changes in one propeller rotation, the possibility of flexible propeller with excellent hydrodynamic performance than enough rigid propeller came into sight.

In this study, two kinds of model propellers are used, which are a metal propeller and an elastically deformable propeller that uses a resin with a smaller flexural modulus than metal. Propeller open water tests, fluctuating pressure measurements and blade deformation measurements were conducted in uniform flow and a wake in cavitation tunnel. As a result, it was found that the flexible composite propeller with high skew had a high risk to lower the thrust, torque and efficiency than the metal propeller by the blade tip deformation, but it had a possibility greatly improved cavitation performance. Further, at the time of the propeller reverse it was found that there was a risk of unstable vibration occurs in blade tip part.

Keywords

Flexible Propeller, Cavitation, Pressure Fluctuation, Open Water Test

1 INTRODUCTION

Marine propellers operating in the wake generate the unsteady propeller fluid forces and cause hull vibrations. The deformations of general metal marine propellers are not considered, because they have enough rigidity. However, marine propellers using the composite material called flexible propeller appeared, by controlling the actively blade deformation in response to load changes in one propeller revolution, the possibility of them with excellent hydrodynamic performance than enough rigid propellers came into sight.

Nakashima Propeller has succeeded in developing the world's first CFRP (Carbon Fiber-Reinforced Plastic) propeller aimed at commercial vessels. It has been reported that excellent characteristics such as "highly efficient", "quiet" and "lightweight" can be achieved by making full use of material properties (Yamatogi & Sakurai 2017).

Many papers related the flexible composite propellers have been published especially in the last decade. Maljaars & Kaminski (2015) has been reporting an overview of hydro-elastic analysis of the flexible propellers. In this paper, it has been shown the survey results that there are few experimental data for flexible composite propellers and few data for verification for fluid-structure interaction computations (FSI) couplings.

Taketani et al (2013) conducted model tests using 20-degrees skew angle composite model propellers with two kinds of Young's modulus in a cavitation tunnel and investigated for the composite propeller performances (propeller characteristics and cavitation performance) under the elastic deformation. As a result, the deformation of propellers has been reduced propeller thrust and torque. Propeller efficiency began to decline with greater deformation. The part of elastic deformation was dominant at the blade tip and this deformation occurred along the direction of thrust and worked such as a forward rake. The cavitation generated after deformation indicated that such deformation reduced loads at the blade tip and affected pitch angles and reduced of pressure fluctuations.

In this study, two kinds of model propellers are used, which are a metal propeller and an elastically deformable propeller that uses a resin with a smaller flexural modulus than metal. Propeller open water tests and fluctuating pressure measurements in uniform flow and in a wake were carried out in cavitation tunnel. The hydrodynamic performance (propeller characteristics and cavitation performance) of the flexible composite marine propeller are shown by comparison with a metal propeller. And the scaling law between deformation and deformation response for flexible composite propellers with deformation is investigated

2 Model Propellers

The model propellers were similar to the highly skewed propeller HSP- II of "SEIUN-MARU I" with 45-degrees skew angle (Kurobe et al 2013). Model propellers manufactured using two kinds of materials were an aluminum alloy propeller (hereinafter, "Metal") and a

flexible composite model propeller made of resin (hereinafter, "Resin"). Table 1 shows the principal particulars of the model propeller, and Table 2 shows the material properties (flexural modulus and Young's modulus) of the model. The model propeller made of aluminum alloy was manufactured by cutting from an aluminum block with a NC machine, and the flexible composite model propeller was manufactured by selective laser sintering method using a 3D printer. The resin material name was PAG3300 (nylon 12 containing 40% glass) The flexible composite model propeller is shown in Figure 1. The tolerances of the offsets on the suction side and the pressure side was less than ±0.05mm for the metal propeller and ±0.30 mm for the resin propeller.

Table 1 Principal particulars of "SEIUN-MARU I" highly skewed model propeller HSP-II.

Diameter [m]	0.250
Boss ratio	0.1972
Pitch ratio at 0.7R	0.9440
Expanded area ratio	0.700
Number of blades	5
Skew angel [deg.]	45

Table 2 Material properties of model propellers.

	Flexural modulus	Young's modulus
Metal	71 GPa	70 GPa
Resin	3.5 GPa	3.8 GPa

Figure 1 Flexible composite highly skewed model propeller HSP-II of "SEIUN-MARU I".

3 EXPERIMENTAL METHOD

Model experiments were conducted in a cavitation tunnel (measurement cross section 710×710 mm) of Mitsubishi Heavy Industries, Ltd. to investigate the propeller open water characteristics in a uniform flow and the propeller open water characteristics and cavitation performance in a wake.

3.1 Test Conditions in Uniform Flow

The propeller advanced ratio J was set to a predetermined value by adjusting the flow velocity U in the cavitation tunnel every propeller rotational speed n, and the propeller open water characteristics (thrust T and torque Q) was measured. The test conditions are shown below. A test matrix of 16 cases has been performed in which 4 different conditions for both n and J have been considered.

- n = 10rps, 15rps, 20rps, 25rps (4 conditions)
- J = 0.6, 0.65, 0.7, 0.75 (4 conditions)

The test results are expressed by the thrust coefficient K_T, torque coefficient K_Q, and propeller efficiency η_P shown in the following equations. Here, D is the propeller diameter and ρ is the fluid density.

$$K_T = \frac{T}{\rho n^2 D^4}\ ,\ K_Q = \frac{Q}{\rho n^2 D^5} \qquad \eta_P = \frac{J}{2\pi}\frac{K_T}{K_Q}\ ,\ J = \frac{U}{nD} \tag{1}$$

3.2 Test Conditions in Wake

In the wake test, a flat plate with the pressure sensors embedded in it for measuring pressure fluctuations was placed in the cavitation tunnel above the model propeller, and a wire mesh simulating the estimated full-scale wake of "SEIUN-MARU" was installed upstream of the propeller. The plate height was adjusted so that the tip clearance gt between the propeller blade tip and the flat plate was gt/D=0.256. The arrangement of the model test is shown in Figure 2.

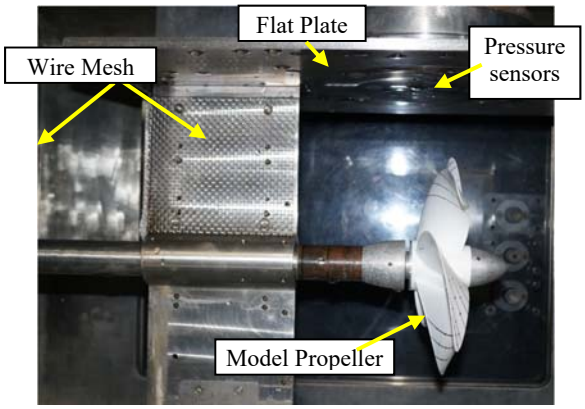

Figure 2 Test arrangements in cavitation tunnel.

The test conditions of propeller open water characteristic measurement and propeller pressure fluctuation measurement in the wake are shown below. In the propeller open water test, measurements were carried out at the pressure in the cavitation tunnel where cavitation did not occur on the propeller.

[Measurement of open water characteristic in wake]

A test matrix of 16 cases has been performed in which 4 different conditions for both n and J have been considered.

- n = 10rps, 15rps, 20rps, 25rps (4 conditions)
- J = 0.6, 0.65, 0.7, 0.75 (4 conditions)

[Measurement of propeller pressure fluctuation]

A test matrix of 6 cases has been performed in which 3 different conditions for n and 2 different propeller load conditions have been considered.

- n = 20rps, 22rps, 25rps (3 conditions)
- K_T = 0.201, $\sqrt{K_T / J}$ = 0.6262 (2 conditions)
- σ_{nc} = 2.99

Here, the cavitation number σ_{nc} and the dimensionless amplitude K_P of the pressure fluctuation are expressed by the following equations using the static pressure Ps at the propeller shaft, the vapor pressure Pv, and the pressure fluctuation ΔP.

$$\sigma_{nc} = \frac{p_s - p_v}{\frac{1}{2}\rho n^2 D^2} \quad , \quad K_P = \frac{\Delta P}{\rho n^2 D^2} \tag{2}$$

4 EXPERIMENTAL RESULTS

4.1 Propeller Open Water Characteristics in Uniform Flow

The propeller open water characteristics due to the change of the propeller rotational speed of the metal propeller and the resin propeller in uniform flow are shown in Figure 4. The metal propeller efficiency tends to increase because the thrust slightly increases and the torque slightly decreases with the increase of the propeller rotational speed. This effect is considered to be the effect of the Reynolds number increase due to the increase in propeller rotational speed.

On the other hand, in the case of resin propeller, both the thrust and torque decrease as the propeller rotational speed increases. When the propeller rotational speed is 20rps or more, the decrease tends to be large in particular. The propeller efficiency is almost constant until the propeller rotational speed is 15rps, but the decrease of the propeller efficiency becomes remarkable when it becomes 20rps or more. It is considered that the resin propeller has a great influence on the propeller open water characteristic because the absolute value of the thrust increases with the increase of the propeller rotational speed and the amount of the propeller blade deformation becomes large.

Figure 3 shows the deformation of the resin propeller at the propeller advanced ratio J=0.6. The amount of deformation at the tip of the propeller increases as the propeller rotational speed increases. In this propeller advanced ratio, the amount of deformation of the propeller blade tip was about 4.5mm at 25rps compared with the case of propeller rotational speed 1rps.

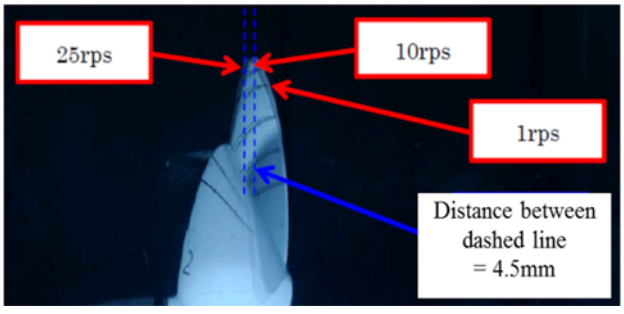

Figure 3 Behavior of resin propeller deformation (J=0.6).

4.2 Propeller Open Water Characteristics in Wake

The propeller open water characteristics due to the change of the propeller rotational speed of the metal propeller and the resin propeller in the wake are shown in Figure 5. As in the case of uniform flow, the metal propeller has a slight increase in thrust and a slight decrease in torque with the increase in propeller rotational speed, so the propeller efficiency tends to increase. This effect is considered to be the effect of Reynolds number increase due to the increase of propeller rotational speed as well as in uniform flow.

On the other hand, in the case of the resin propeller, as in uniform flow, with increasing propeller rotational speed, the tendency to decrease both thrust and torque is the same. But when the propeller rotational speed exceeds 20rps, the phenomenon observed in the uniform flow in which the thrust and torque sharply decrease cannot be seen. As a result of comparing the propeller efficiency with the propeller loading ($\checkmark K_T / J$) base, the efficiency of the resin propeller is several percent lower than that of the metal propeller even in the wake as well as in the uniform flow.

Although the propeller thrust in the wake is higher than that in the uniform flow at the same rotational speed and propeller advanced ratio, the reason why the thrust and torque of the resin propeller in the uniform flow is greatly reduced when the propeller rotation speed becomes 20rps or more is discussed. The Highly Skewed Propeller of "SEIUN-MARU" (HSP-II) is designed as a tip unloaded propeller with wake distribution taken into consideration. When the propeller is operated in a uniform flow, the inflow velocity near the blade tip is relatively low compared to that in the wake at the same propeller advanced ratio, and therefore the angle of attack becomes large. Because of this, the degree of propeller loading near the blade tip increases, so it is expected that the amount of deformation of the blade tip increases in resin propellers. Due to this effect, when the propeller rotational speed becomes 20rps or more in uniform flow, the deformation amount of the tip of the resin propeller becomes large, and it is considered that the rapid decrease of thrust and torque occurred.

4.3 Propeller Pressure Fluctuations in Wake

Comparison of the primary and secondary components of the blade frequency of the pressure fluctuations just above the propeller due to the change of propeller rotational speed for the metal propeller and resin propeller in the wake are shown in Figure 6 (K_T is constant) and Figure 7 ($\checkmark K_T / J$ is constant). The pressure fluctuations of the metal propeller are almost constant regardless of the propeller rotational speed, but both the primary component and the secondary component of the pressure fluctuations of the resin propeller are more than 50% lower than those of the metal propeller. The reduction effect of pressure fluctuations increases as the propeller rotational speed increases.

The mechanism for reducing propeller pressure fluctuations of the resin propeller is considered to be mainly due to the reduction of the amount of cavitation generated on the blade surface by the elastic deformation of the blade tip. The deformation of the blade tip is considered to be bending to the low-pressure side (suction side) of the blade surface and torsional deformation that reduces the pitch angle of the blade tip. Among these phenomena, the reduction of the blade tip pitch angle has

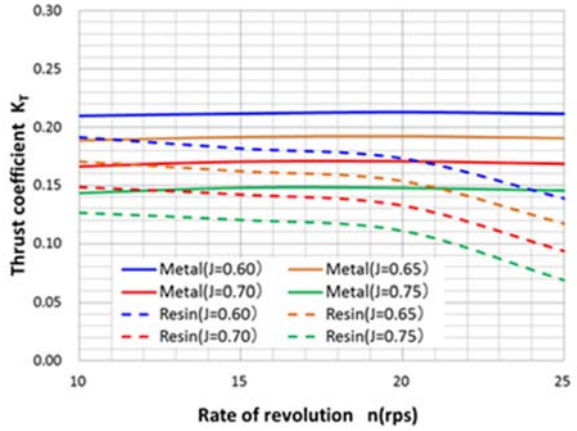

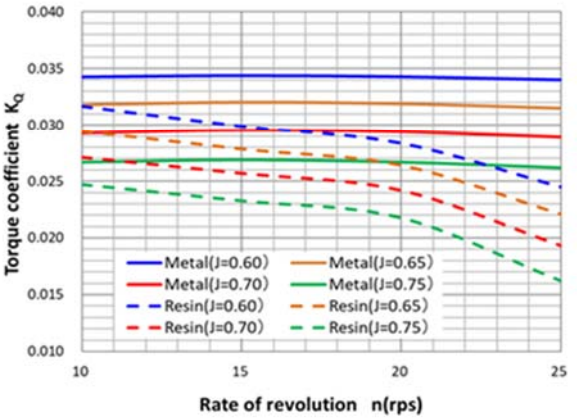

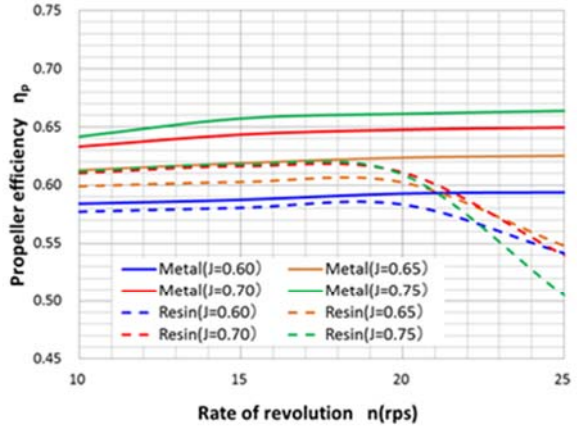

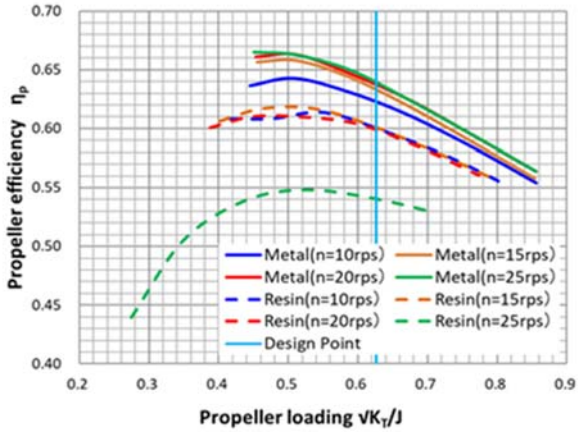

Figure 4 Comparison of propeller open water characteristics in uniform flow.

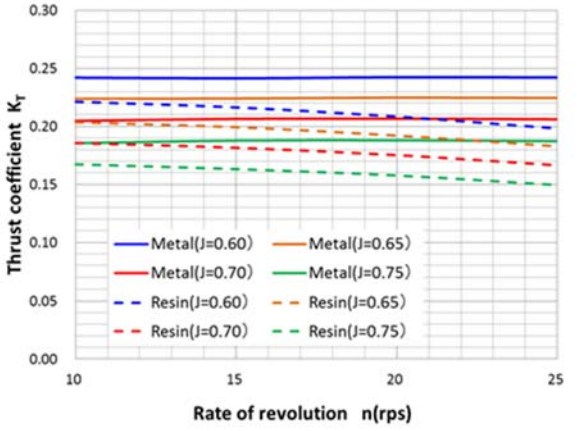

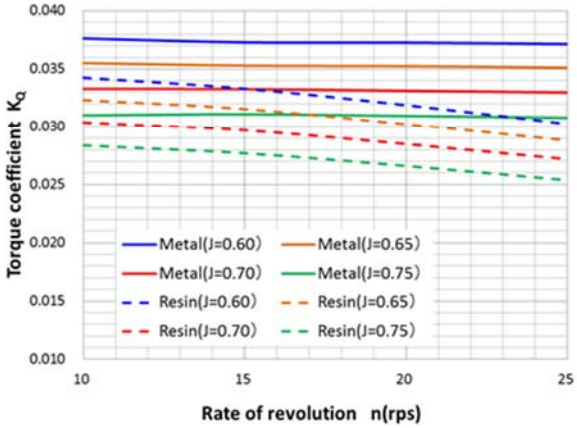

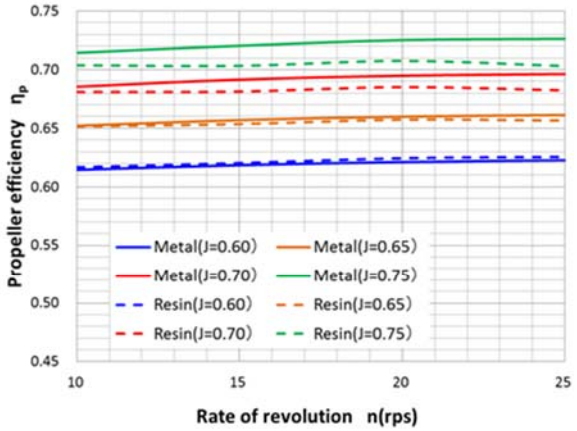

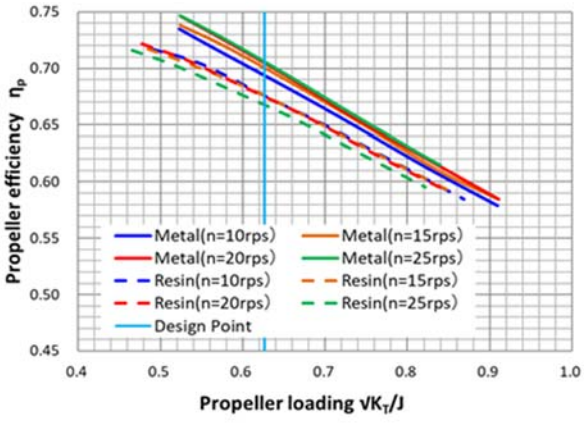

Figure 5 Comparison of propeller characteristics in wake.

the effect of reducing the amount of cavitation, since it acts in the direction of reducing the angle of attack.

Figure 8 shows the cavitation sketch that occurs on the blade surface of a metal propeller and a resin propeller at a propeller operating point K_T =0.201, a propeller rotational speed n =25rsp, and a propeller phase angle θ of 40 °. Figure 9 shows photographs of cavitation pattern at propeller phase angles of 30 °, 40 °, and 50 ° in the resin propeller. It can be seen that the amount of cavitation generated on the resin propeller is greatly reduced compared to the metal propeller. In addition, the range of propeller phase angle at which cavitation occurs is smaller in the resin propeller compared to the metal propeller.

A simple image processing is performed with commercial software using image data recording the deformation of the resin propeller taken during the test, the pitch angle changes of the resin propeller blade tip at the propeller operating point KT =0.201 and the propeller phase angle θ=300 °. The results due to the change of propeller rotational speed are shown in Figure 10. It can be seen that the amount of reduction of the pitch angle increases as the propeller rotational speed increases. In this propeller, there is no big difference in the amount of reduction of the pitch angle until the propeller radius position 0.9R (90% radius position), but the reduction amount of the pitch angle at 0.95R of the blade tip is larger than other radius positions. The pitch angle was reduced by about 1.7 ° at a propeller rotational speed of 25rps.

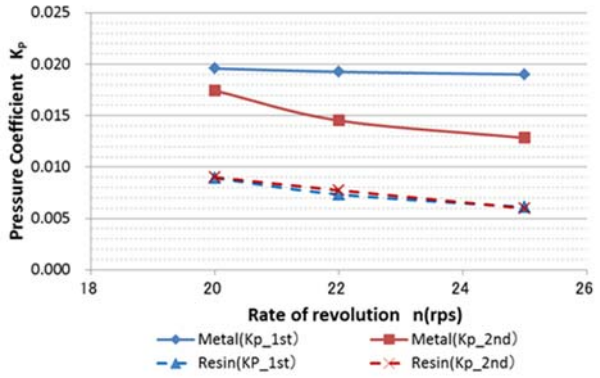

Figure 6 Comparison of pressure fluctuations (K_T=0.201).

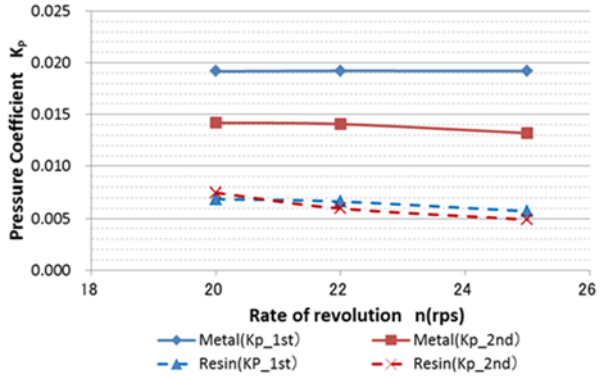

Figure 7 Comparison of pressure fluctuations ($\sqrt{K_T/J}$ =0.626).

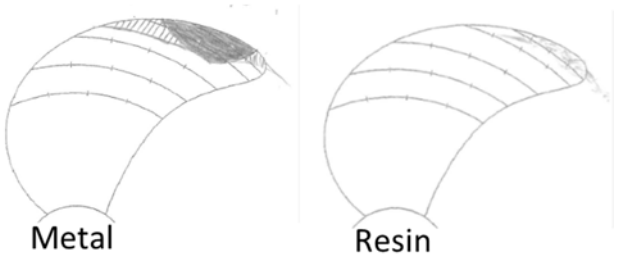

Figure 8 Comparison of cavitation patterns (K_T =0.201, n =25rps, θ =40°).

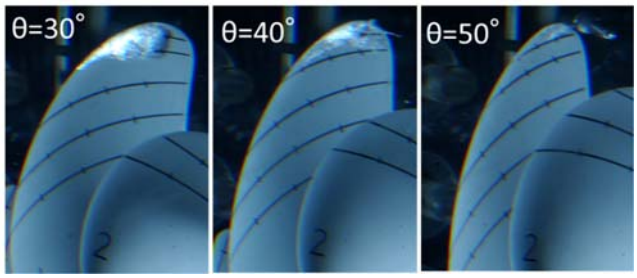

Figure 9 Comparison of cavitation patterns for resin propeller (K_T =0.201, n =25rps).

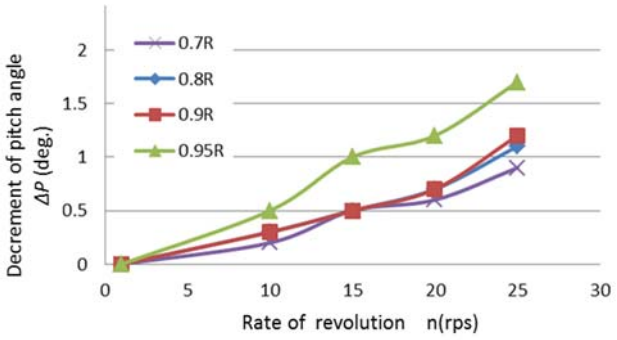

Figure 10 Comparison of decrement of pitch angle for resin propeller (K_T =0.201, θ=300°).

4 UNSTABLE VIBRATION DURING PROPELLER REVERSE ROTATION

When stopping the ship, the variable pitch propeller changes the pitch angle without changing the propeller rotational direction, but the fixed pitch propeller reverses the propeller rotational direction. Figure 11 shows an example of the unstable vibration generated at the propeller blade tip when the resin propeller is reversely rotated in the wake at the propeller advanced ratio J= -0.4 and the propeller rotational speed n= -10rps. Unstable large deformation was observed at the propeller tip. The skew of this resin propeller is backward skew at normal rotation, but it is forward skew at reverse rotation. In the case of backward skew, the blade tip is deformed in the direction of decreasing the pitch angle by the fluid force acting on the blade tip, but in the case of forward skew, the blade tip is deformed in the direction of increasing the pitch angle. Therefore, the large deformation of the blade tip observed at the time of reverse rotation is considered to be the deformation caused by the divergence.

It is considered that the state of the unstable vibration phenomenon at the blade tip as seen this time is different depending on the rigidity of the blade material and the

propeller shape (especially, skew angle), so it is necessary to investigate in detail the generation mechanism and the safety on strength. In addition, it is considered necessary to investigate self-excited vibration such as the flutter.

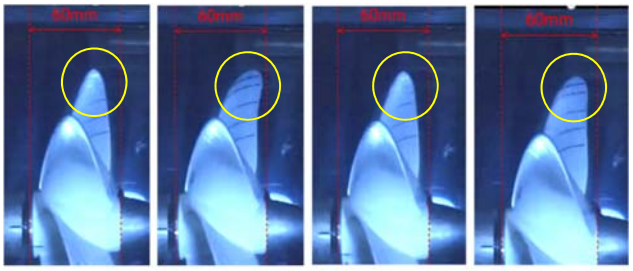

Figure 11 Unsteady deformation of the foil at the time of propeller reverse in wake (*J*= -0.4, *n* = -10rps).

5 SCALING LAW OF FLEXIBLE COMPOSITE MODEL PROPELLER

The scaling law between deformation and deformation response for flexible composite propellers with deformation is investigated. It is shown that it is possible to estimate the material properties of the model propeller that can make the deformation and deformation response similar from the Young's modulus and the density of material and the diameter and operating conditions for the full-scale propeller.

5.1 Scaling Law on Deformation and Deformation Response

5.1.1 Scaling Law

The deformation response is examined by the natural frequency. Consider the deformation and vibration of the beam to simplify the problem. The amount of deformation y at the end of the cantilever is expressed by Equation (3).

$$y = \frac{PL^3}{3EI} \tag{3}$$

Here, P is the load, L is the length of the beam, E is the Young's modulus, and I is the second moment of area. The propeller diameter is D, the propeller rotational speed is n, and the fluid density is ρ. If the propeller shape and the operating condition, i.e., the thrust force T, are similar, the following equations are obtained.

$$P = T \propto \rho n^2 D^4 \ , \ L = D \ , \ I \propto D^4 \tag{4}$$

In order to make the deformation similar, it is enough if the value shown by Equation (5) obtained by substituting Equation (4) into Equation (3) is equal between the model propeller and the full-scale propeller.

$$\frac{y}{D} \propto \frac{\rho n^2 D^4 D^3}{E D^4 D} = \frac{\rho n^2 D^2}{E} \tag{5}$$

Next, consider the vibration of the cantilever. The natural frequency f of a cantilever beam is expressed by Equation (6) using the material density ρ_m of the beam.

$$f \propto \frac{1}{L^2}\sqrt{\frac{EI}{\rho_m L^2}} \tag{6}$$

In order for the deformation response to be similar between the model propeller and the full-scale propeller, it is sufficient if the ratio between the propeller rotational speed n shown in Equation (7) and the natural frequency f of the beam is equal between the model propeller and the full-scale propeller.

$$\frac{f}{n} \propto \frac{1}{nD^2}\sqrt{\frac{ED^4}{\rho D^2}} = \frac{1}{nD}\sqrt{\frac{E}{\rho}} \tag{7}$$

5.1.2 Material property

From Equation (5), in order to make the deformation similar between the model propeller and the full-scale propeller, it is necessary to reduce the material rigidity of the model. At present, it is difficult to product a model propeller as a composite material with a laminated structure, so it is conceivable to use a resin material as in the model propeller used in this research.

5.2 Trial Calculation

If the Young's modulus and elastic density of the full-scale flexible composite propeller are 35GPa and 50GPa, and the material density is 2000kg/m^3, for the propeller of "SEIUN-MARU I ", the results of calculating the Young's modulus required for the model material using Equations (5) and (7) are shown in Figure 12.

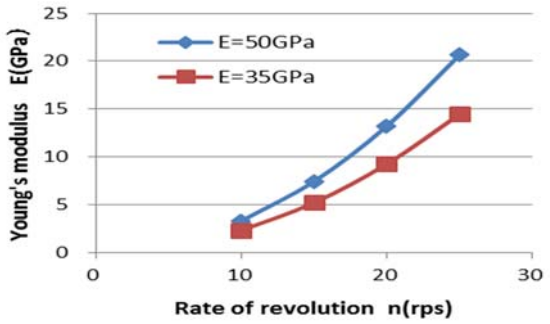

Figure 12 Necessary Young's modulus for model propeller.

The required Young's modulus changes significantly when the model propeller rotational speed is changed during the tank test. Since the Young's modulus of the model propeller carried out in this study is 3.5GPa, the model propeller rotational speed, which is in a state of deformation similar to that of the full-scale propeller, is about 10rps. If it is desired to carry out propeller rotational speed of about 20rps in model test, Young's modulus of model material needs to be 10GPa or more, so it is necessary to make model propeller from resin material containing fiber with high Young's modulus. Currently, fiber-filled resin materials have a material with a Young's modulus of 10GPa or more.

6 CONCLUSIONS

In order to understand the hydrodynamic performance of the flexible composite marine propellers, the open water characteristics and cavitation performance of the metal model propeller and the flexible composite model propeller were experimentally investigated for the high skew propeller of " SEIUN-MARU I". As a result, the following findings were obtained.

1) The flexible composite propeller with high skew has a high risk to lower thrust, torque and efficiency under the same operating condition than the metal propeller due to blade tip deformation, but it has a possibility greatly improved cavitation performance.
2) Knowing the Young's modulus and density of a full-scale propeller, propeller diameter and operating conditions, it is possible to estimate the material properties of a flexible composite model propeller that can make deformation and deformation response similar.
3) It was found that there was a risk of unstable vibration occurs in blade tip part at the time of the propeller reverse condition. In the future, it is necessary to investigate the relationship between both the rigidity of the blade material and propeller shape and the unstable vibration phenomena such as divergence and flutter.

ACKNOWLEDGEMENTS

This study was supported by JSPS KAKENHI Grant Number JP18H01649. In conducting the study, we would like to express our sincere gratitude to Mr. Takano and Mr. Kubo of Mitsubishi Heavy Industries, Ltd., who cooperating with experiments.

REFERENCES

Kurobe, Y., Ukon, Y., Koyama, K. & Makino, M. (1983). 'Measurement of Cavity Volume and Pressure Fluctuations on a Model of the Training Ship "SEIUN-MARU" with Reference to Full Scale Measurement,' Ship Research Institute Report, Vol. 20, No. 6.

Maljaars, P.J. & Kaminski, M.L. (2015). 'Hydro-elastic Analysis of Flexible Propellers: An Overview,' Fourth International Symposium on Marine Propulsors, Austin, Texas, USA.

Taketani, T., Kimura, K., Ando. S. & Yamamoto, K. (2013). 'Study on Performance of a Ship Propeller Using a Composite Material,' Third International Symposium on Marine Propulsors, Launceston, Tasmania, Australia.

Yamatogi, T. & Sakurai, T. (2017). 'Research and Development of CFRP Propellers,' Journal of the Japan Institute of Marine Engineering, Vol. 52, No. 2.